



## Numerical Modelling of a Valveless Impedance Pump with Various Pinch Locations

Mohamad Mazwan Mahat<sup>1,\*</sup>, Muhammad Sabaruddin Ahmad Jamali<sup>1</sup>, Salmiah Kasolang<sup>1</sup>

<sup>1</sup> School of Mechanical Engineering, College of Engineering, Universiti Teknologi MARA, 40450 Shah Alam, Selangor, Malaysia

### ABSTRACT

Microfluidics devices offers reliable transport mechanism to drive fluid within a microscale flow. This research work aims to identify the characteristic of flow in valveless impedance pump which uses acoustic impedance mismatch to drive flow using numerical simulations. The focus of the studies is designing a well performed pump where the required displacement of elastic wall can still be achieved even when the force applied in different locations and also a mechanism that requires low input current. Shear rate resulting from the pumping mechanism were measured at different input boundary conditions. Important parameters such as pinch location can affect the direction of the velocity magnitude and shear rate. It is found that the maximum shear rate occurred at 2 mm pinch location at  $400 \text{ s}^{-1}$ . Hence, the pump design from this study can be used as the best application for microfluidic systems where a high pumping amount is desired.

### Keywords:

Impedance pump; microfluidic;  
frequency; excitations; elastic tube

Received: 3 August 2022

Revised: 5 October 2022

Accepted: 7 October 2022

Published: 21 October 2022

## 1. Introduction

A vital component of the human body is the circulatory system, which is made up of blood arteries and the heart. It operates throughout the body by delivering sufficient nutrients to distant organs and helping the lungs take in oxygen and discharge waste products like carbon dioxide. Once the circulation system fails, it will cause the rest of the organs in the body to malfunction. The primary part that will be affected is the heart. As a result, the chronic heart disease will lead to the heart failure. An importance of heart is a situation in which the heart unable to pump sufficient blood throughout the body. This is because the force energy of the heart is insufficient to perform the circulatory operation. Because the heart valves have not formed at this stage of development, the net flow of blood through the heart must be propelled by a separate process [1]. However, many patients died and suffered while waiting for heart transplant due to lack of donor. In United States of America, there is only heart assists device namely as New Generation Heart Mate II that had been approved by the United States Food and Drug Administration to be applied as a temporary supporting

\*Corresponding Author

E-mail address: [mazwan@uitm.edu.my](mailto:mazwan@uitm.edu.my)

<https://doi.org/10.37934/araset.28.2.135147>

system before heart donation process take place as well as for destination therapy or long-term. The concept of novel pumping mechanism inspired by the embryonic heart structure [2,3].

Furthermore, the device controlled by the impeller axially and the use of rotating disc pumps. Thus, it leads to the damage of blood cells flowing through the impeller. In this research, a study on nonlinear multiphase flow and transport in heterogeneous porous media was conducted. The major reference for this research is Gerhart Liebau concept. Many researchers have carried out analytical [4] or computational studies [5] in a bid to better comprehend the mechanisms at work in the Liebau problem of valveless pumping in open [6] or closed-loop [7] systems. It is believed that Liebau pumping plays a crucial role in heart development and several other physiological processes [8]. Numerous distinctive features of the net flow produce by a Liebau effect pump are easily describe by wave dynamics [9,10]. For instant, the connection between compression frequency and flow rate is non-linear [11]. Liebau suggested that viscosity, inertia and elasticity affected the parameters measured in the device. The pumping mechanism that was proposed by Liebau [12] is still the subject of interest across a wide range of disciplines, including physiology, engineering, physics, and biomedical research, due to the complexity of the mechanism and the fact that it is dependent on a large number of variables [13]. Liebau conducted the initial research on the phenomena of valveless pumping to comprehend the mechanism behind the blood circulatory system [14]. The main reason why it created as valveless due to prevent the problems that arise by using a valves with laminar flow in pipes which  $Re \leq 2300$  [15].

They may be used in the subject areas of biology, chemistry, medical science, and biomedical engineering [16]. Valveless pump also is useful for cost effective space limited applications due to their basic geometry and straightforward assembly. Valveless pumping is an innovative new technology for creating or increasing net flow in both macro and micro scale devices [17]. An impedance pump is a kind of valveless pumping mechanism in which an elastic tube and a stiff tube with a different impedance are connected. Impedance pump are another term for Liebau effect pumps [6,18,19]. The elastic tube portion is continually subjected to an unequal compression, which might result in wave reflection and unidirectional flow [20]. The experimental investigation of the behaviour of impedance pump shown that flows are extremely responsive to duty cycle and pinching frequency. The simplicity of the excitation effort required to operate an impedance pump and the absence of seals and blade are its advantages. Pulsatile flow created by an impedance pump will be superior to a simple flow for application like mixing fluids [21].

With the advance of technology nowadays the possibility of survival among the patient increased. However, the current ventricular assist devices still have some limitation. The current generation of mechanical pumps requires thinning of the blood (or anticoagulation) to prevent the formation of blood clots. These clots can cause dysfunction of the pump itself, or more typically, can embolize into the circulation and cause a transient ischemic attack, stroke, or lack of blood flow to a limb or vital organ. This pumping concept offers a low energy, low noise alternatively at both micro and macro scales. Valveless pumps are easy to construct and require few moving parts. Moreover, there are lots of characteristic of impedance pump that can be discovered. By obtaining the flow rate for each different case, the best parameters which may provide the optimum flow rate can be identified. Instead of peristaltic action, longitudinal standing with patterns provides the net flow. All of the research assumed a homogeneous cylindrical tube, with thin walls in most cases [22]. By just adjusting the phase between them, several pinches allow for simple control of the size and direction of the net flow [23]. A complicated series of waves is created by pinching the flexible tube completely or partially at an off-centre location relative to its ends on a regular basis [10].

One of the potential approaches to overcome the situation is to use mechanical device that can assist blood flow in patient suffering from hearth problem such as the loss of blood pressure and

low cardiac output. The device is called Ventricular Assist Device VAD that is important device used to help heart failure [24]. Multiple different mechanical devices for long-term circulatory support have been developed, ranging from total artificial hearts to ventricular assist devices (VADs). The main purpose of a VAD is to unload the failing heart and help maintain forward cardiac output and vital organ perfusion [25]. Originally introduced as a temporary bridge to recovery and then as a bridge to transplantation, VADs have involved into permanent or “destination” therapy for a growing number of patients with refractory heart failure. A ventricular assist device (VAD) is a mechanical circulatory device that is used to partially or completely replace the function of a failing heart. Some VADs are intended for short term use, typically for patients recovering from heart attacks or heart surgery, while others are intended for long-term use (months to years and in some cases for life), typically for patients suffering from congestive heart failure.

Valveless pumping mathematical models can be represented by either a closed loop system or an open tube system [26]. We offer a three-dimensional model of valveless pumping in a closed loop system in this study [27]. When it comes to the computation of the elastic forces exerted by the immersed boundary on the fluid, most methods of Peskin's immersed boundary technique are explicit [28]. Most immersed boundary approaches use an explicit approach to calculate the elastic forces on the structure's known configuration at each time step. Because the fluid-structure interaction is a stiff problem in nature, an explicit IB technique has a severe time step size limitation. The time step must be modest enough to preserve numerical stability [29]. Implicit numerical approaches are frequently preferred to address the inherent stiffness in fluid-structure interaction situations.

Many efforts have been made in recent years to build implicit or semi-implicit IB approaches [30]. However, the majority of these implicit approaches are impractical for real-world application situations. The authors have recently developed a lattice-Boltzmann-based two-dimensional (2D) implicit immersed boundary approach [31]. A previous work produced a one-dimensional model by approximating the Navier-Stokes equations, which included the effects of viscosity, energy loss, and gravity. The flow is quantitatively represented by a one-dimensional approximation of the Navier-Stokes equations [32]. Because of the preceding models' simplifications and assumptions, only a limited understanding of the pumping mechanism was attainable [33]. Our approach is based on an efficient Navier-Stokes solver that employs the fractional-step method and a static Cartesian grid structure. The fluid motion on a Eulerian grid and the structural motion on a moving Lagrangian grid are solved independently, and their interaction is modelled via momentum forcing. A net flow is generated inside the valveless pump by periodic pinching of the elastic tube at an asymmetric location with respect to its ends.

## **2. Methodology**

### *2.1 Experimental Technique and Geometrical Modelling of Elastic Tube*

For validation purpose, an experiment was setup with several procedures design to meet the basic configuration. The material and equipment of the experiment is shown in Figure 1 and connected as shown in figure 1. Total length of 200 mm elastic tube with the thickness of 1 mm were joined together with a rigid tube. Then, water was fully filled into the whole circuit via T-tubing barb. The pincher location was set placed about 2 mm from the left side of the elastic tube. Before started the experiment, the voltage of DC motor was set up to 2.0 V. The electrical power supply was switched on to let the pincher press the elastic tube. When the pincher pressed the elastic tube section, the water inside the rigid tube will flow through the flow meter. The flow rates of the flow meter were recorded. After that, repeat the step using of 3 mm thickness of elastic tube with

different applied voltages of 3.0, 4.0, 5.0 and 6.0 V respectively. Lastly, the steps are repeated by using 260 mm length of elastic tube.

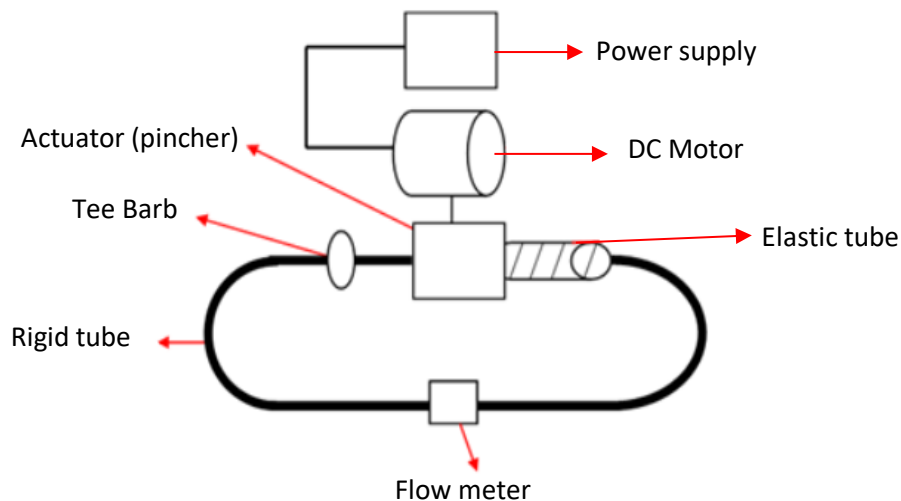


**Fig. 1.** Model Configuration

**Table 1**  
 Geometrical setup

Part	Parameter	
Elastic tube	Outer Diameter, mm	30.0
	Thickness, mm	1.0 and 3.0
	Length, mm	200.0 and 260.0
Actuator	Length, mm	150.0
	Diameter, mm	10.0
	Thickness, mm	10.0
Electrical DC motor	Voltage, V	2.0, 3.0, 4.0, 5.0 and 6.0

## 2.2 Simulation Set Up and Boundary Condition

Next to the experimental investigations, the fluid flow simulation was simulated with CFD Module which is COMSOL Multiphysics. The overall simulation set up was based on physical conditions and geometry statistics in Table 2. In view of computational analysis, the element type of the meshing for elastic tube is tetrahedral with element numbers of 1-3 M elements. Table 2 below shows the summarizes of the geometry statistics of numerical analysis employed in this investigation. The fluid flow inside the elastic tube is changing with various type of liquid with different density and viscosity. The properties of the fluid are listed in table 3 below.

**Table 2**  
 Geometry statics of Numerical Analysis

<b>Physical conditions</b>	
Fluid	water
Fluid volume ( $\pi \times r^2 \times h$ ):	
• Elastic tube	$\pi \times (15)^2 \times 200$
Elastic tube material	Plastic
<b>Geometry statistics</b>	
Space dimension	2
Number of domains	2
Number of boundaries	7
Number of vertices	6
<b>Computational elements</b>	
Element type	Tetrahedral
Number of elements	1-3 M elements

**Table 3**  
 The properties of five different fluids

Fluid	Density (kg/m <sup>3</sup> )	Viscosity (Pa.s)
Water	998.2	0.001002
Glycerin Solution 1 (GS1)	1043	0.00135
Glycerin Solution 2 (GS2)	1046.8	0.00138
Glycerin Solution 3 (GS3)	1076.8	0.00267
Glycerin Solution 4 (GS4)	1086.1	0.00281

### 2.3 Meshing Geometry of Computational Domain

Users may run these simulations for various fluid flows using the sophisticated CFD Module, an add-on for COMSOL Multiphysics. These include two-phase flow, thin film flow, rotating machinery, non-Newtonian flow, turbulent flow, laminar and creeping flow, and non-Newtonian flow. Computational fluid dynamic COMSOL Multiphysics was used to simulate 3D model for pincher process for the water pipe. COMSOL Multiphysics was utilized to build the meshing geometry and solving the governing equations in this study. However, this solution also can be solved using ANSYS FEA software [34]. In order to assess the impact of turbulent viscous sublayers, Figure 2 depicts the application of a tetrahedral mesh to the elastic tube surface with inflated mesh layers positioned close to the walls using a non-uniform adaptive technique at a rate of 1.1 enhancement. As shown in Figure 2, the mesh is gradually refined until a finer mesh is reached along the wall directly in contact with the fluid. These techniques make it possible to predict velocity fluctuations and recirculation zones along the walls with greater accuracy.

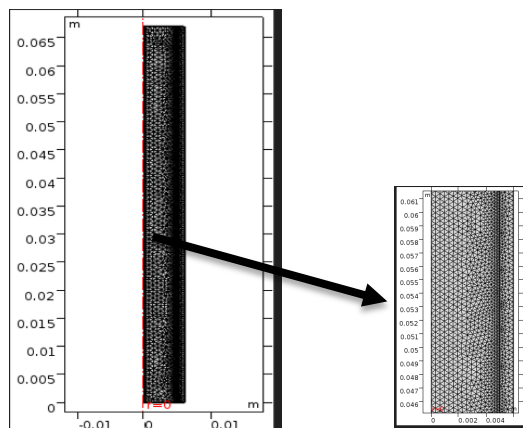


Fig. 2. Mesh Generation

## 2.4 Numerical Analysis

This convergence study examined six turbulence models in order to select the optimal and most efficient model for future simulations. The average relative error for each iteration can be calculated using the following formula:

$$R_C = \frac{1}{n.m} \sum_{i=1}^m \sum_{j=1}^n \left| \frac{(P_{i,j}^{S+1} - P_{i,j}^S)}{P_{i,j}^{S+1}} \right| \quad (1)$$

$P$  represents parameters such as temperature and velocity,  $s$  represents the number of iterations, and  $i, j$  represents the grid position. Both the momentum and energy equations are solved using the upwind difference method of the second order. When the sum of the residuals in an energy equation is less than  $10^6$ , the solution is deemed convergent. The threshold for convergence of relative residuals in continuity and momentum equations is  $10^4$  [35]. By comparing the error values, it was determined that the  $k - \omega$  SST had the lowest error for outlet velocity (0.00216 percent) and temperature (0.00094 percent). This finding is consistent with that of Y. Yoon et al. [36]. The three-dimensional Navier-Stokes equations are as follows:

$$\begin{aligned} \nabla(\rho \vec{U}u) &= -\frac{\partial p}{\partial x} + \frac{\partial \tau_{xx}}{\partial x} + \frac{\partial \tau_{yx}}{\partial y} + \frac{\partial \tau_{zx}}{\partial z} \\ \nabla(\rho \vec{U}v) &= -\frac{\partial p}{\partial y} + \frac{\partial \tau_{xy}}{\partial x} + \frac{\partial \tau_{yy}}{\partial y} + \frac{\partial \tau_{zy}}{\partial z} \\ \nabla(\rho \vec{U}w) &= -\frac{\partial p}{\partial z} + \frac{\partial \tau_{xz}}{\partial x} + \frac{\partial \tau_{yz}}{\partial y} + \frac{\partial \tau_{zz}}{\partial z} \end{aligned} \quad (2)$$

$U$  is the fluid velocity, while  $u, v,$  and  $w$  are variables in the  $x, y,$  and  $z$  directions, respectively.  $\rho$  is the density of the fluid,  $p$  is the pressure, and  $\tau_{xz}$  is the viscous stress tensor. The fluid flow is described by the incompressible Navier-Stokes equations:

$$\nabla u = 0,$$

$$\left(\frac{\partial u}{\partial t} + \rho u \cdot \nabla u\right) = -\nabla p + \nabla \cdot \mu * (\nabla u + (\nabla u)) + f,$$

$$f = \int F \delta^2(z - Z) ds,$$

$$F = -\kappa_t((Z) - L) + \kappa_c \left(\frac{\partial Z}{\partial s^2}\right). \quad (3)$$

where  $\rho$  denotes the density (SI unit: kg/m<sup>3</sup>),  $\sigma$  is elastic strain tension,  $u$  the velocity (SI unit: m/s),  $\mu$  the viscosity (SI unit: Pa·s),  $F$  is singular force density,  $Z$  is immersed boundary,  $L$  is targeted of immerse boundary,  $\kappa_c$  is stiffness constant,  $s$  is a material point of immersed boundary and  $p$  the pressure (SI unit: Pa).

$$A = -\frac{a}{4} \left(\cos\left(\frac{2\pi}{d\beta} t\right) - 1\right) (\cos 2\pi - 1), \quad (4)$$

where  $a$  is the amplitude of the pump.  $f$  is the frequency of the oscillation. Velocity profile is assumed corresponding to a fully developed flow given by:

$$u(r, z) = u_{\max} \left(1 - \frac{z^2}{r^2}\right) \text{ and } v(r, z) = 0 \text{ at } r = 0, \quad (5)$$

For the fluid simulation, the boundary condition at the inlet and the outlet assumes that the total stress is zero, that is:

$$n \cdot [-pI + \mu(\nabla u + (\nabla u))] = 0 \quad (6)$$

The volumetric flow rate at any instant  $t$ , compute a boundary integral over the pipe's inlet and outlet boundary:

$$V_{in} = - \int_{S_{in}} 2\pi r (n \cdot u) ds$$

$$V_{out} = \int_{S_{out}} 2\pi r (n \cdot u) ds \quad (7)$$

The inlet and outlet boundaries are horizontal so:

$$n \cdot u = n_x u + n_y v \quad (8)$$

To track how much fluid is conveyed through the outlet during the cycle:

$$V_{pump}(t) = \int_0^t V_{out} dt' \quad (9)$$

### 3. Results

#### 3.1 Velocity Magnitude Across the Elastic Tube at Different Pinch Location

The velocity magnitude across the elastic tube at different pinch location is shown in Figure 3. The magnitude of velocity vector gives the speed of fluid flow inside the elastic tube. The results of magnitude of velocity shown that it is decreases as the arc length of the elastic velocity increases. The highest velocity magnitude is at 1 m/s for 3 mm of pinch location. Then, the velocity magnitude decreases until 0 m/s at arc length 0.004 m. Based on Figure 3, we can see that at 4 mm pinch location, the velocity magnitude of fluid flow is minimum which is 0.75 m/s compared to others. However, the velocity magnitude decreases until 0 m/s at arc length 0.0053 m higher than the others.

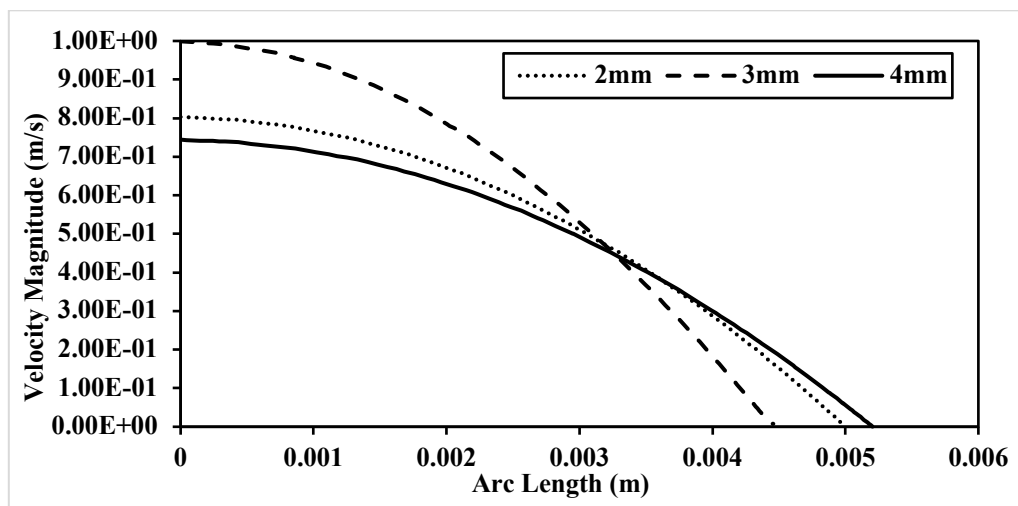


Fig. 3. Velocity magnitude across the elastic tube at different pinch location

#### 3.2 Pressure across the Elastic Tube at Different Pinch Location

When analysing the effectiveness of the fluid flow in the elastic tube, the pressure distribution across the elastic tube is one of the main key factors. Based on Figure 4 shown below, all the pressure distribution for different pinch location gives similar results as it is decreasing as the arc length increases. The close loop system demonstrated that the pressure were not sustain [18]. The maximum pressure is  $1.6 \times 10^8$  Pa at 3 mm pinch location while the minimum pressure is  $9.0 \times 10^7$  Pa at 4 mm pinch location.

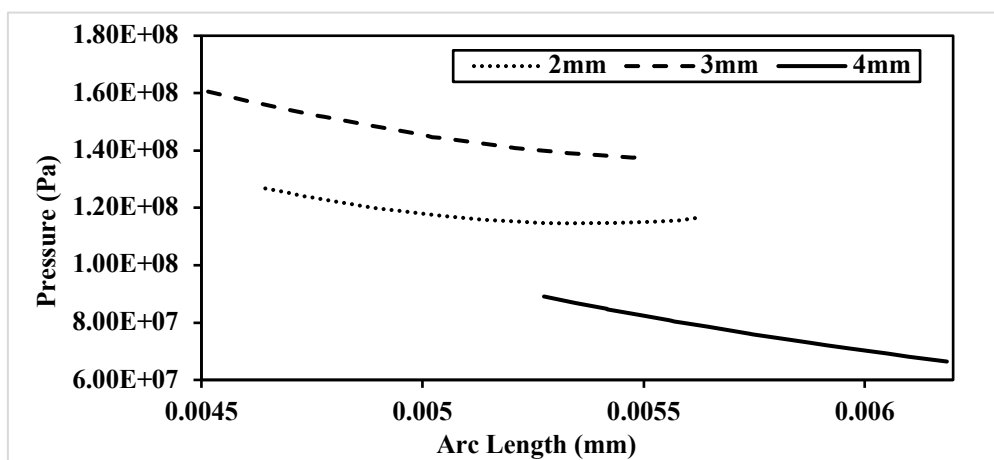


Fig. 4. Pressure distribution across the elastic tube at different pinch location

### 3.3 Shear Rate across the Elastic Tube at Different Pinch Location

The pace at which a fluid is sheared or worked while flowing is known as the shear rate. Technically speaking, it is the speed at which fluid laminar or layers pass one another. Both the geometry and the flow's speed affect shear rate. Shear rate is crucial since it may have a big impact on how viscous the materials are. Based on Figure 5 below, the pattern of shear rate for all results is approximate with each other. It is shown an uneven line of graph where it is increasing as the arc length increases.

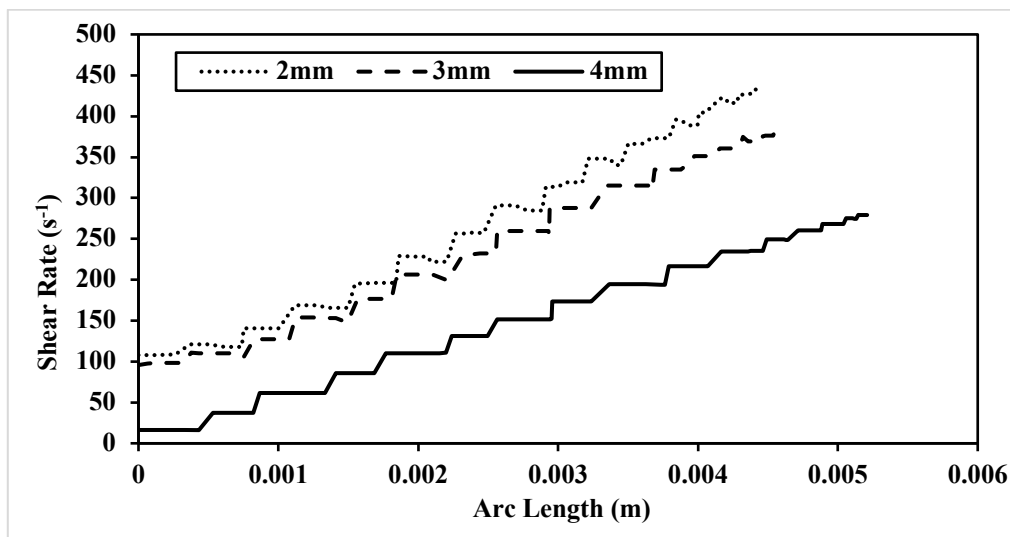


Fig. 5. Shear rate across the elastic tube at different pinch location

### 3.4 Validation and Verification

Preliminary calculations were made on an elastic tube with the same dimensions as those investigated by Hickerson *et al.*, [9] in order to assess the computational model and methodology employed in the current numerical simulation. Figure 6 below shows the comparison of pressure between current modelling findings and experimental data. The correlation between the experimental data and our predicted results is fairly good, supporting the correctness of the physical model and the numerical approach.

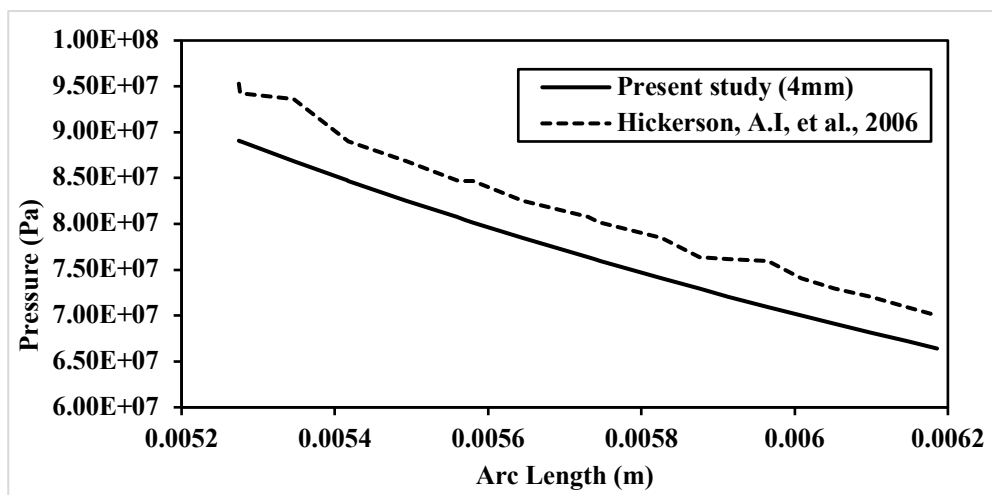


Fig. 6. Validation and Verification

### 3.5 Velocity Magnitude across the Elastic Tube with Different Liquid

Based on Figure 7 below, it is shown that the water has higher velocity magnitude compared to others fluid which is at 1.01 m/s. This is due to the glycerin solution has higher viscosity and denser than the water. Thus, it takes more power to get it going in the same speed as water. The lowest velocity magnitude from all the liquids is glycerin solution 4 which at 0.74 m/s.

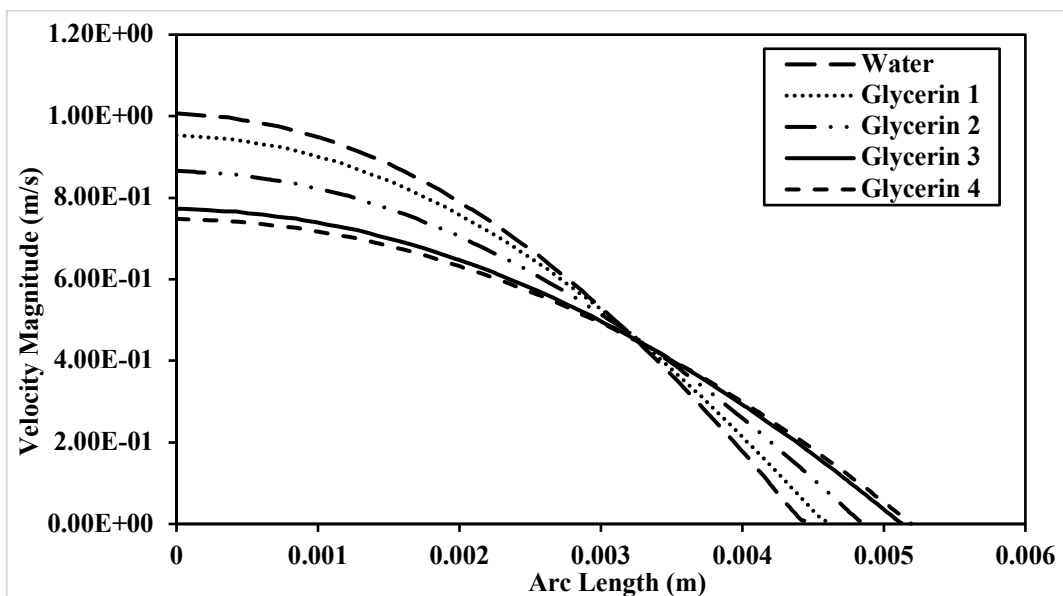


Fig. 7. Velocity magnitude across the elastic tube with different fluid

### 3.6 Velocity Magnitude across the Elastic Tube with Same Fluid different Pinch Location

Based on Figure 8 below, it is showing the results of velocity magnitude across the elastic tube with same fluid but different pinch location. The fluid that been used is glycerin solution 1 with density and viscosity at 1043 kg/m<sup>3</sup> and 0.00135 Pa.s respectively. The results shown that the velocity magnitude of glycerin solution 1 at 2 mm pinch location is higher than the 3 mm and 4 mm pinch location. The velocity magnitude of glycerin solution 1 at 4 mm pinch location is lowest compared to the others.

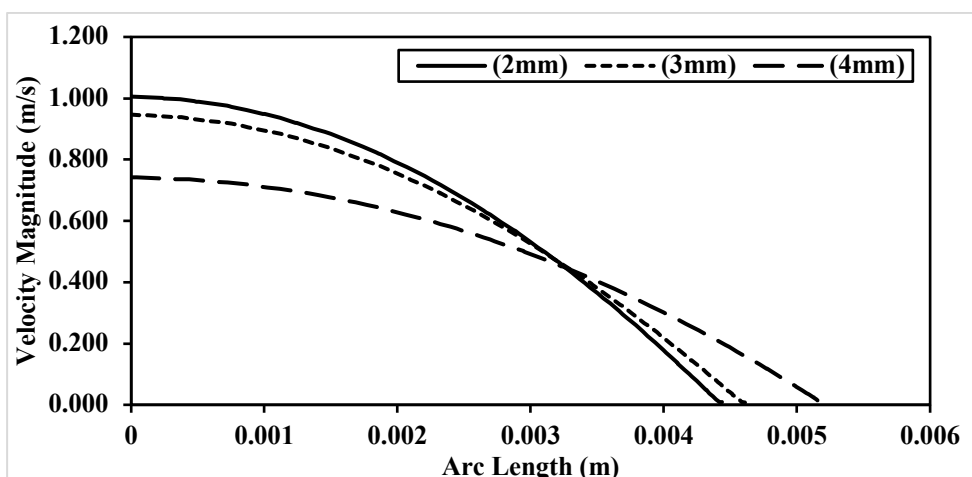
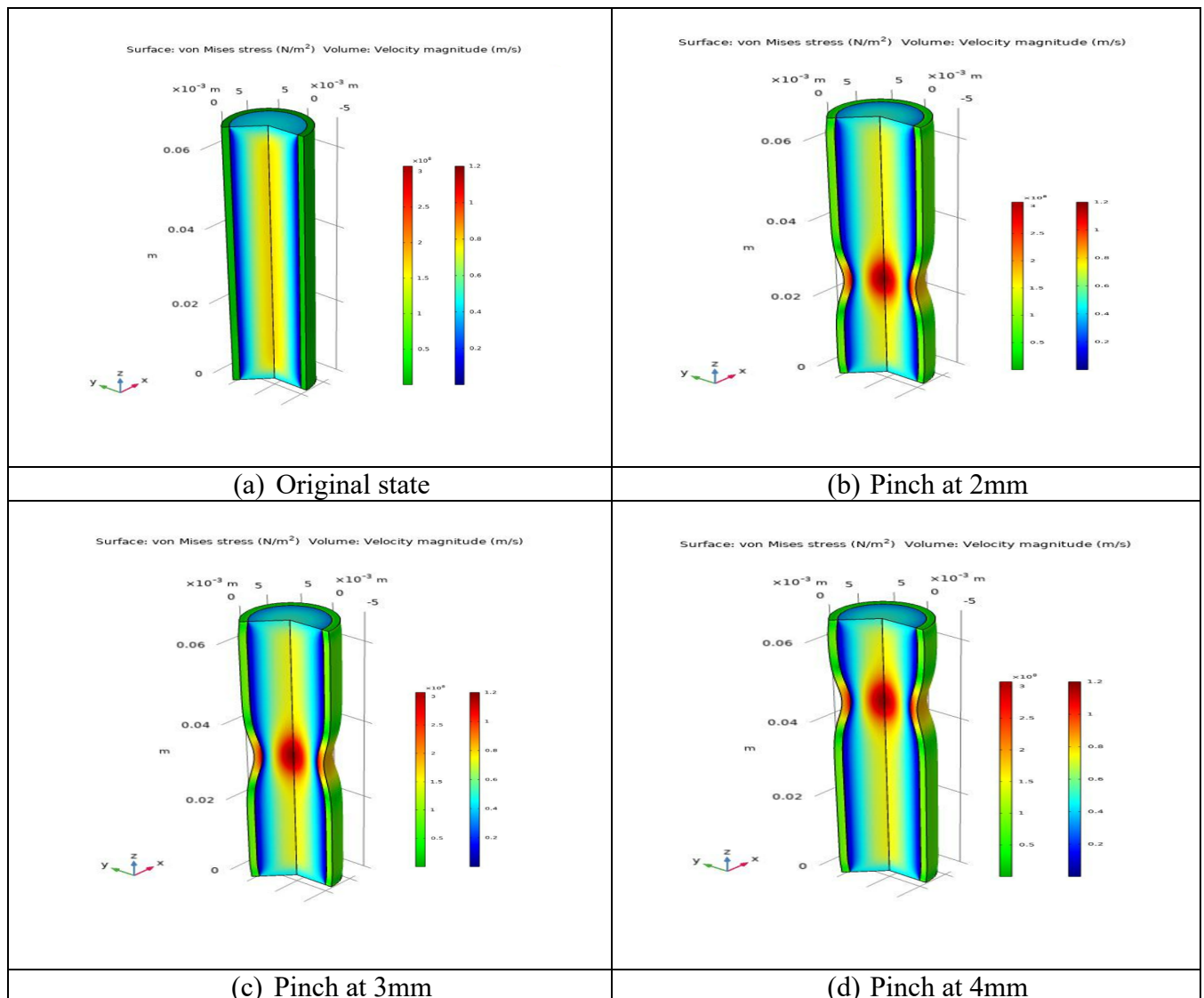


Fig. 8. Velocity magnitude across the elastic tube with same fluid different pinch location

### 3.7 Von Mises Stress Distribution across the Surface Area of Elastic Tube at Different Pinch Location

The Von mises stress distribution over the surface of elastic tube is shown in figure 9(a)-(d). The most intriguing feature of the Figures is that the stress source's center, which corresponds to the area of the elastic tube that being pinched, exhibits the maximum stress. On the other hand, it is noticeable that the elastic tube's other than the region that being pinched experiences a progressive drop in stress distribution as it has no force devoted on that region. For instance, in Figure 9 (b), the higher stress that being recorded is at red region which corresponding to the  $3 \times 10^8 \text{ N/m}^2$  while the minimum stress is at  $0.2 \times 10^8 \text{ N/m}^2$ .



**Fig. 9.** Von Mises Stress contour of elastic tube at different pinch location

## 4. Conclusions

In this study of numerical modelling of a valveless impedance pump with various pinch location, we have shown the effect of pinch location towards flow behaviour in valveless pump through the velocity magnitude and pressure distribution across the elastic tube. There are several identifying characteristics of impedance driven flows that can be used to correctly identify impedance driven pumping processes. An impedance pump requires only one active element which are not in

the centre along the length of the wave propagation portion. Moreover, by aiming to investigate the wall shear stress distribution on elastic tube wall based upon different input boundary conditions, we came out with the pattern shear rate across the elastic tube at different pinch location.

### Acknowledgement

The authors would like to acknowledge the School of Engineering, Universiti Teknologi MARA (UITM) Shah Alam and Ministry of Higher Education in providing financial support via the Fundamental Research Grant Scheme No FRGS/1/2019/TK03/UITM/02/20.

### References

- [1] Battista, Nicholas A., Andrea N. Lane, and Laura A. Miller. "On the dynamic suction pumping of blood cells in tubular hearts." In *Women in mathematical biology*, pp. 211-231. Springer, Cham, 2017. [https://doi.org/10.1007/978-3-319-60304-9\\_11](https://doi.org/10.1007/978-3-319-60304-9_11)
- [2] Loumes, L., I. Avrahami, and M. Gharib. "Resonant pumping in a multilayer impedance pump." *Physics of Fluids* 20, no. 2 (2008): 023103. <https://doi.org/10.1063/1.2856528>
- [3] Wen, Chih-Yung, Shi-Jung Yeh, Kuok-Pong Leong, Wei-Shen Kuo, and Howard Lin. "Application of a valveless impedance pump in a liquid cooling system." *IEEE transactions on components, packaging and manufacturing technology* 3, no. 5 (2013): 783-791. <https://doi.org/10.1109/TCPMT.2012.2230298>
- [4] Lee, V. C. C., Y. A. Abakr, and K. C. Woo. "Performance evaluation of multi-stage open-loop impedance pump." *International Journal of Mechanical and Materials Engineering* 12, no. 1 (2017): 1-9. <https://doi.org/10.1186/s40712-017-0079-1>
- [5] Hickerson, Anna Iwaniec. *An experimental analysis of the characteristic behaviors of an impedance pump*. California Institute of Technology, 2005.
- [6] Wen, C-Y., and H-T. Chang. "Design and characterization of valveless impedance pumps." *Journal of Mechanics* 25, no. 4 (2009): 345-354. <https://doi.org/10.1017/S1727719100002835>
- [7] Shin, Soo Jai, and Hyung Jin Sung. "Three-dimensional simulation of a valveless pump." *International journal of heat and fluid flow* 31, no. 5 (2010): 942-951. <https://doi.org/10.1016/j.ijheatfluidflow.2010.05.001>
- [8] Sarvazyan, Narine. "Building Valveless Impedance Pumps From Biological Components: Progress and Challenges." *Frontiers in physiology* (2022): 2407. <https://doi.org/10.3389/fphys.2021.770906>
- [9] Hickerson, Anna Iwaniec, and Morteza Gharib. "On the resonance of a pliant tube as a mechanism for valveless pumping." *Journal of Fluid Mechanics* 555 (2006): 141-148. <https://doi.org/10.1017/S0022112006009220>
- [10] Avrahami, I. D. I. T., and Morteza Gharib. "Computational studies of resonance wave pumping in compliant tubes." *Journal of Fluid Mechanics* 608 (2008): 139-160. <https://doi.org/10.1017/S0022112008002012>
- [11] Hiermeier, Florian, and Jörg Männer. "Kinking and torsion can significantly improve the efficiency of valveless pumping in periodically compressed tubular conduits. Implications for understanding of the form-function relationship of embryonic heart tubes." *Journal of Cardiovascular Development and Disease* 4, no. 4 (2017): 19. <https://doi.org/10.3390/jcdd4040019>
- [12] Hiermeier, Florian, and Jörg Männer. "Kinking and torsion can significantly improve the efficiency of valveless pumping in periodically compressed tubular conduits. Implications for understanding of the form-function relationship of embryonic heart tubes." *Journal of Cardiovascular Development and Disease* 4, no. 4 (2017): 19. <https://doi.org/10.3390/jcdd4040019>
- [13] Davtyan, Rubina, and Narine A. Sarvazyan. "Output of a valveless Liebau pump with biologically relevant vessel properties and compression frequencies." *Scientific reports* 11, no. 1 (2021): 1-9. <https://doi.org/10.1038/s41598-021-90820-4>
- [14] Shin, Soo Jai, Cheong Bong Chang, and Hyung Jin Sung. "Simulation of a valveless pump with an elastic tube." *International journal of heat and fluid flow* 38 (2012): 13-23. <https://doi.org/10.1016/j.ijheatfluidflow.2012.08.003>
- [15] T. Hadush, "Flow in pipes Flow in pipes," *Fluid Mech.*, pp. 321-398, 2004.
- [16] Sarvazyan, Narine. "Thinking outside the heart: Use of engineered cardiac tissue for the treatment of chronic deep venous insufficiency." *Journal of cardiovascular pharmacology and therapeutics* 19, no. 4 (2014): 394-401. <https://doi.org/10.1177/1074248413520343>
- [17] Carmigniani, Remi A., Michel Benoit, Damien Violeau, and Morteza Gharib. "Resonance wave pumping with surface waves." *Journal of Fluid Mechanics* 811 (2017): 1-36. <https://doi.org/10.1017/jfm.2016.720>
- [18] Hickerson, Anna Iwaniec, Derek Rinderknecht, and Morteza Gharib. "Experimental study of the behavior of a valveless impedance pump." *Experiments in fluids* 38, no. 4 (2005): 534-540. <https://doi.org/10.1007/s00348->

[005-0946-z](#)

- [19] Lee, VC-C., Y. A. Abakr, and K-C. Woo. "Valveless pumping using a two-stage impedance pump." *Frontiers of Mechanical Engineering* 8, no. 3 (2013): 311-318. <https://doi.org/10.1007/s11465-013-0270-x>
- [20] A Abd Razak, Azli, Mohd Mohamad, and Nazirul Rosli. "Experimental Study on Net Flow Rate Generation Inside Closed Loop Mechanical Circulatory System Using Impedance Pump." *International Journal of Engineering & Technology* 7, no. 10.14419 (2018). <https://doi.org/10.14419/ijet.v7i3.11.15927>
- [21] Lee, Vincent Chieng-Chen, Yousif Abdalla Abakr, and Ko-Choong Woo. "Experimental investigation of a multi-stage impedance pumping system." In *AIP Conference Proceedings*, vol. 1440, no. 1, pp. 1206-1211. American Institute of Physics, 2012. <https://doi.org/10.1063/1.4704338>
- [22] Kozlovsky, Pavel, Moshe Rosenfeld, Ariel J. Jaffa, and David Elad. "Dimensionless analysis of valveless pumping in a thick-wall elastic tube: Application to the tubular embryonic heart." *Journal of Biomechanics* 48, no. 9 (2015): 1652-1661. <https://doi.org/10.1016/j.jbiomech.2015.03.001>
- [23] Rosenfeld, Moshe, and Idit Avrahami. "Net flow rate generation by a multi-pincher impedance pump." *Computers & Fluids* 39, no. 9 (2010): 1634-1643. <https://doi.org/10.1016/j.compfluid.2010.05.016>
- [24] Abdelshafy, Mahmoud, Kadir Caliskan, Goksel Guven, Ahmed Elkoumy, Hagar Elsherbini, Hesham Elzomor, Erhan Tenekecioglu, Sakir Akin, and Osama Soliman. "Temporary right-ventricular assist devices: A systematic review." *Journal of Clinical Medicine* 11, no. 3 (2022): 613. <https://doi.org/10.3390/jcm11030613>
- [25] Rodriguez, Limaël E., Erik E. Suarez, Matthias Loebe, and Brian A. Bruckner. "Ventricular assist devices (VAD) therapy: new technology, new hope?." *Methodist DeBakey cardiovascular journal* 9, no. 1 (2013): 32. <https://doi.org/10.14797/mdcj-9-1-32>
- [26] Jung, Eunok, Sookkyung Lim, Wanho Lee, and Sunmi Lee. "Computational models of valveless pumping using the immersed boundary method." *Computer methods in applied mechanics and engineering* 197, no. 25-28 (2008): 2329-2339. <https://doi.org/10.1016/j.cma.2008.01.024>
- [27] Manopoulos, Christos, Sokrates Tsangaris, and Dimitrios Mathioulakis. "Net flow generation in closed-loop valveless pumping." *Proceedings of the Institution of Mechanical Engineers, Part C: Journal of Mechanical Engineering Science* 234, no. 11 (2020): 2126-2142. <https://doi.org/10.1177/0954406220904110>
- [28] Hao, Jian, and Luoding Zhu. "A three dimensional implicit immersed boundary method with application." *Theoretical and Applied Mechanics Letters* 1, no. 6 (2011): 062002. <https://doi.org/10.1063/2.1106202>
- [29] Zhu, Luoding. "Viscous flow past a flexible fibre tethered at its centre point: vortex shedding." *Journal of Fluid Mechanics* 587 (2007): 217-234. <https://doi.org/10.1017/S002211200700732X>
- [30] Rinderknecht, Derek. *Development of a microimpedance pump for pulsatile flow transport-Part: Flow characteristics of the microimpedance pump. Part 2: A systematic study of steady and pulsatile transport in microscale cavities*. California Institute of Technology, 2008.
- [31] Taira, Kunihiko, and Tim Colonius. "The immersed boundary method: a projection approach." *Journal of Computational Physics* 225, no. 2 (2007): 2118-2137. <https://doi.org/10.1016/j.jcp.2007.03.005>
- [32] Zislin, Victor, and Moshe Rosenfeld. "Impedance pumping and resonance in a multi-vessel system." *Bioengineering* 5, no. 3 (2018): 63. <https://doi.org/10.3390/bioengineering5030063>
- [33] Timmermann, Stine, and Johnny T. Ottesen. "Novel characteristics of valveless pumping." *Physics of Fluids* 21, no. 5 (2009): 053601. <https://doi.org/10.1063/1.3114603>
- [34] Wang, Yu-Hisang, Yao-Wen Tsai, Chien-Hsiung Tsai, Chia-Yen Lee, and Lung-Ming Fu. "Design and analysis of impedance pumps utilizing electromagnetic actuation." *Sensors* 10, no. 4 (2010): 4040-4052. <https://doi.org/10.3390/s100404040>
- [35] Tariq, Adeel, Khurram Altaf, Syed Waqar Ahmad, Ghulam Hussain, and T. A. H. Ratlamwala. "Comparative numerical and experimental analysis of thermal and hydraulic performance of improved plate fin heat sinks." *Applied Thermal Engineering* 182 (2021): 115949. <https://doi.org/10.1016/j.applthermaleng.2020.115949>
- [36] Yoon, Young Chan, Dong Rip Kim, and Kwan-Soo Lee. "Cooling performance and space efficiency improvement based on heat sink arrangement for power conversion electronics." *Applied Thermal Engineering* 164 (2020): 114458. <https://doi.org/10.1016/j.applthermaleng.2019.114458>